AAS 12-247

INCLUDING VELOCITY UNCERTAINTY IN THE PROBABILITY OF COLLISION BETWEEN SPACE OBJECTS

Vincent T. Coppola*

While there has been much research on computing the probability of collision between space objects, there is little work on incorporating velocity uncertainty into the computation. We derive the formula from first principles, including both position and velocity uncertainty. Moreover, trajectories will evolve according to differential equations and not by approximating the relative motion. The end result is a 3-dimensional integral over time on the surface of a sphere. We show that the formula recovers the classic formula in the limit as the velocity uncertainty approaches zero. Finally, the results produced using the new formula will be compared to the results of Monte Carlo simulations.

INTRODUCTION

The derivation of the probability of collision formula goes back at least as far as the work of Foster and Estes[1] who developed a formula applicable to the ISS. Improvements and extensions were made by Chan,[2,3] Alfano,[4,5] Khutorovsky et al.,[6] Akella and Alfriend,[7] Patera,[8] Oltrogge,[9] and others. Chan's book[3] serves as resource for many aspects of spacecraft collision probability, including computational considerations. Alfano's works[5,10,11] also include development of computational methods for determining conjunction probability in short-term and long-term encounters.

The relative position uncertainty is the primary focus of these derivations; any velocity uncertainty, if considered at all, only leads to the relative position uncertainty changing with time: it is not an integral part of the formula itself. During long-term encounters, initial velocity uncertainty would lead to significantly different trajectories even when starting at the same position. The differing trajectories should then have some impact on whether a collision occurs and affect the probability of collision value.

In this paper, we derive the formula for the probability of collision between space objects from first principles. The two objects will be modeled as having both position and velocity uncertainty (as the orbit determination process would model them as having) and their trajectories will evolve according to differential equations describing their motion (and not approximated as lines or by the CW equations). At each stage in the derivation, the requisite assumptions will be identified.

The derivation begins by connecting the Monte-Carlo simulation process for computing the probability of collision to a formula that integrates a probability density function over time. The critical insights are that (i) the spatial integral of import is the surface of a sphere fixed in the relative position space of the two objects; and (ii) a time integral arises by considering the flux of trajectories entering the sphere over time. Both constructs follow naturally. The sphere arises from the definition of the probability of collision. The flux arises from a transformation of variables into spherical

*Sr. Astrodynamics Developer, Analytical Graphics Inc., 220 Valley Creek Blvd, Exton PA, 19341.

coordinates. This is different from the discussion in Khutorovsky et al.[6] and Akella and Alfriend[7] in that only the *influx* will be seen to be of importance, not the outflux.

Before simplification, the expression for the probability of collision is a 12-dimensional integral: the 12 dimensions arise from the state of each object being 6 dimensional (3 each for position and velocity). Surprisingly, 9 of the dimensions can be integrated analytically leaving only a 2-dimensional integral over a sphere and a 1-dimensional integral over time. The expression results from mild assumptions (e.g., the covariances of the two objects are uncorrelated and Gaussian; each relative trajectory is in collision only once); neither the short encounter duration assumption nor the linear motion assumption has been made at this point however. While the expression is not an analytic formula, it is quite simple to compute numerically. The time integral can be performed using Simpson's rule; integration routines on a spherical surface have been developed since the late 1950's, with the best known being those developed by Lebedev.[12] Both algorithms are well-suited for parallelization using multiple threads and/or GPUs.

After deriving the fundamental expression, we will show that the result reduces to the classic short encounter result in the limit as the velocity uncertainty approaches zero. We then compare the results of the new formula with the results of Monte Carlo simulations, for both short-term and long-term encounters. The new formula is shown to be both accurate and fast to compute.

DERIVATION

We are interested in finding the probability that the range between two space objects will become less than some specified threshold R within a time of interest.

> *Definition.* Given initial conditions for two objects at time t_0, a radius threshold $R > 0$, and a maximum time of interest $T > 0$, two objects are said to collide if $\exists t \in [t_0, t_0{+}T]$ such that $\|\mathbf{r}(t)\| \leq R$, where $\mathbf{r}(t)$ is relative range vector between the objects at time t.

This is a simple view of the term 'collision'. To actually determine whether two objects collide or not, one would need to know the attitude and location of each of its parts and then determine whether any of the parts would come into contact. The attitude and configuration of each object is not usually known, especially for debris, which is why this simpler definition is used. The value R is usually chosen as the sum of the hard body radii* of the two objects.

Note. While there are just a few key concepts used in the derivation, the mathematical detail can appear daunting at times. Details have been provided to help the reader see the validity of the end result. The derivation brings together many different mathematics fields (e.g., integration, dynamical systems, probability theory, normal distributions). Guidance is provided to the reader to put these pieces into place to solve the larger puzzle. The derivation ends with the probability of collision formula defined by Eq. (38).

Note. The appendices provide background information on probability density functions and Gaussian distributions that may help acclimate the reader to issues discussed in the derivation. Appendix A contains several lemmas that will be used in the derivation to simplify many of the results.

*The hard body radius of an object is the radius of the smallest sphere that would encompass the entire object.

Fundamental Formula

The dynamical model for the two objects is given by

$$
\begin{aligned}
\frac{d\mathbf{X}}{dt} &= \mathbf{f}(\mathbf{X}, t)\ , \mathbf{X}(t_0) = \mathbf{X}_0 \qquad (1)\\
\mathbf{X} &= (\mathbf{x}_a, \mathbf{x}_b)\ ,\\
\mathbf{x}_i(t_0) &= \mathbf{x}_{i_0},\ i = a, b,
\end{aligned}
$$

where $\mathbf{x}_i = (\mathbf{r}_i, \mathbf{v}_i)$ with $\mathbf{r}_i$ being the position of object i and $\mathbf{v}_i$ its velocity. The relative motion will be denoted by $\mathbf{x} = (\mathbf{r}, \mathbf{v})$ where

$$
\begin{aligned}
\mathbf{x} &= \mathbf{x}_b - \mathbf{x}_a\ ,\\
\mathbf{r} &= \mathbf{r}_b - \mathbf{r}_a\ ,\\
\mathbf{v} &= \mathbf{v}_b - \mathbf{v}_a\ .
\end{aligned}
$$

While the motion is deterministic, the initial conditions are uncertain*. The corresponding probability density function $\rho_0(\mathbf{X}_0; t_0)$ has the property that for any domain Γ for $\mathbf{X}_0$, the probability that $\mathbf{X}_0 \in \Gamma$ is

$$P(\mathbf{X}_0 \in \Gamma) = \int\limits_{\Gamma} \rho_0(\mathbf{X}_0; t_0) d\mathbf{X}_0\ . \qquad (2)$$

Note that the initial condition space spanned by $\mathbf{X}_0$ is 12-dimensional. The mean initial condition will be denoted by $(\boldsymbol{\mu}_{a_0}, \boldsymbol{\mu}_{b_0}) = (\boldsymbol{\mu}_{\mathbf{r}_{a_0}}, \boldsymbol{\mu}_{\mathbf{v}_{a_0}}, \boldsymbol{\mu}_{\mathbf{r}_{b_0}}, \boldsymbol{\mu}_{\mathbf{v}_{b_0}})$. We will use the term 'nominal trajectory' to describe the solution to Eq. (1) with initial conditions given by $(\boldsymbol{\mu}_{a_0}, \boldsymbol{\mu}_{b_0})$. In general, the nominal trajectory at time t is not the mean value of $\mathbf{X}$ at time t. (The nominal trajectory is the mean trajectory when the state equations in Eq. (1) describe a linear system.)

Let $V \subseteq \mathbb{R}^{12}$ be the set of initial conditions for which a collision occurs. By definition, the probability of collision is then

$$P = \int\limits_{V} \rho_0(\mathbf{X}_0; t_0) d\mathbf{X}_0\ . \qquad (3)$$

The definition of P given by Eq. (3) is the mathematical description of computing the probability using a Monte Carlo technique. In a Monte Carlo simulation, initial conditions $\mathbf{X}_0$ would be sampled, and trajectories for both objects would be computed (perhaps through numerical integration of Eq. (1)) over the time interval $[t_0, t_0 + T]$. These trajectories would then be investigated to determine whether a collision occurred at some time t. If they do produce a collision, then $\mathbf{X}_0 \in V$. The probability is then determined from the sampled results. Of course, many samples must be taken to insure accuracy (see Alfano[11]). For a 12-dimensional system the cost to perform the Monte Carlo simulation can be prohibitive, given the accuracy needed from the computation.

Transforming Variables using the State Equations

The difficulty in evaluating Eq. (3), of course, is the determination of the set V. Define V_0 as the set of initial conditions $\mathbf{X}_0$ for which $\|\mathbf{r}(t_0)\| \leq R$, that is, the set of initial conditions that

*The initial state of a space object is determined by an orbit determination process that aims to produce an estimate for the state given various measurements. While both the dynamical model and the measurements may be assumed to be uncertain, we shall not consider dynamical model uncertainty in this paper.

are within the specified range R at the initial time t_0. Define $V_I = V - V_0$, i.e., the set of initial conditions having a collision at some time $t > t_0$. From Eq. (3), we find $P = P_0 + P_I$ where

$$P_0 = \int_{V_0} \rho_0(\mathbf{X}_0; t_0) d\mathbf{X}_0 \quad \text{and} \quad P_I = \int_{V_I} \rho_0(\mathbf{X}_0; t_0) d\mathbf{X}_0 \ . \tag{4}$$

We shall concentrate most of our efforts at evaluating P_I because in many cases P_0 can be well-approximated as 0. In particular, if the TCA* for the nominal trajectory occurs at $t^* \gg t_0$ then it may be the case that the objects are so widely separated at t_0 that $\rho_0(V_0; t_0) \approx 0$ leaving $P_0 \approx 0$. In any case, P_0 can be computed since V_0 is fully known:

$$V_0 = \{\mathbf{X}_0 \ | \ \|\mathbf{r}_0\| \leq R\} \text{ where } \mathbf{r}_0 = \mathbf{r}(t_0) \ . \tag{5}$$

No initial condition $\mathbf{X}_0 \in V_I$ meets the range criterion for collision at t_0, but will meet it at some later time $t > t_0$. Consider a subset of initial conditions $\Omega_t \subset V_I$ whose trajectories satisfying Eq. (1) *first* meet the conditions for collision at time t, i.e.,

$$\Omega_t = \{\mathbf{X}_0 \ | \ \|\mathbf{r}(t)\| = R, \text{ but } \|\mathbf{r}(\tau)\| > R \ \forall\tau \ \in [t_0, t)\}. \tag{6}$$

Every initial condition $\mathbf{X}_0 \in V_I$ must be in exactly one set Ω_t for some $t \in (t_0, t_0 + T]$ and thus

$$V_I = \bigcup_{t \in (t_0, t_0+T]} \Omega_t. \tag{7}$$

The set Ω_t is still difficult to characterize; however, its definition in Eq. (6) suggests that P_I is simpler to evaluate in new variables.

The dynamical flow given by Eq. (1) creates a t-parametric transformation $\Phi_t : \mathbf{X}_0 \mapsto \mathbf{X}(t)$, i.e., $\mathbf{X} = \Phi(\mathbf{X}_0, t; t_0)$. Applying the transformation to the set Ω_t, we find

$$\Lambda_t = \Phi_t(\Omega_t) = \{\mathbf{X}(t) \ | \ \|\mathbf{r}(t)\| = R, \text{ but } \|\mathbf{r}(\tau)\| > R \ \forall\tau \ \in [t_0, t)\}. \tag{8}$$

Thus, the set V_I under the transformation of variables Φ_t becomes

$$U_I = \bigcup_{t \in (t_0, t_0+T]} \Phi_t(\Omega_t) = \bigcup_{t \in (t_0, t_0+T]} \Lambda_t \ . \tag{9}$$

The transformation of the integrand follows from the conservation of probability on differential elements†:

$$\rho_0(\mathbf{X}_0; t_0) d\mathbf{X}_0 = \rho(\mathbf{X}, t; t_0) d\mathbf{X} \tag{10}$$

where $\rho(\mathbf{X}, t; t_0)$ is the probability distribution function at time t. Thus, in the transformed variables,

$$P_I = \int_{U_I} \rho(\mathbf{X}, t; t_0) d\mathbf{X} = \int_{t_0}^{t_0+T} \int_{\Lambda_t} \rho(\mathbf{X}, t; t_0) d\mathbf{X} \ . \tag{11}$$

---

*Time of Closest Approach.

†See Appendix B for a discussion of the effect of a variable transformation on the probability of density function.

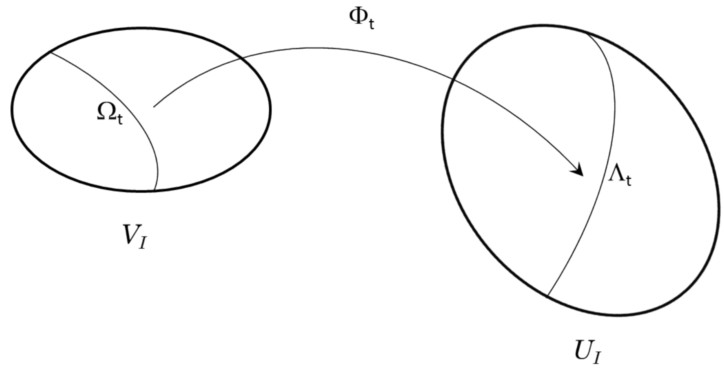

Figure 1. Transforming coordinates using $\Phi_t : \mathbf{X}_0 \mapsto \mathbf{X}(t)$ maps Ω_t into Λ_t at each time $t > t_0$.

Transforming Variables using the Relative Motion

More care must be taken concerning $d\mathbf{X}$ in Eq. (11) than at first appears. Given a time t, the integration is first performed over Λ_t, which is an 11-dimensional set. During that integration, $r(t) = \|\mathbf{r}(t)\|$ remains constant with value R. It is natural then to use coordinates for U_I that respect Λ_t, and thus use the coordinates $(\mathbf{x}_a, \mathbf{x}) = (\mathbf{r}_a, \mathbf{v}_a, \mathbf{r}, \mathbf{v})$, with $\mathbf{r} = \mathbf{r}(r, \phi, \theta)$ expressed in spherical coordinates. On Λ_t, the coordinate r has the constant value R, while the other 11 elements vary. Letting $d\mathbf{A}_{\Lambda_t}$ represent the 'area' element on Λ_t, we find

$$\begin{aligned} d\mathbf{X} = d\mathbf{x}_a\, d\mathbf{x}_b = d\mathbf{x}_a\, d\mathbf{x} &= d\mathbf{x}_a\, d\mathbf{r}\, d\mathbf{v}\ , \\ &= R^2 \cos\theta\, d\mathbf{x}_a\, d\mathbf{v}\, dr\, d\theta\, d\phi\ \triangleq d\mathbf{A}_{\Lambda_t}\, dr, \\ &= \left|\frac{dr}{dt}\right| d\mathbf{A}_{\Lambda_t}\, dt = \left|\mathbf{v}\cdot\hat{\mathbf{r}}\right| d\mathbf{A}_{\Lambda_t}\, dt, \end{aligned} \tag{12}$$

where $\hat{\mathbf{r}}(\phi, \theta)$ is the unit vector along $\mathbf{r}$. The absolute value arises from the standard change of variables formula for differential elements,

$$d\boldsymbol{\xi} = \left|\det \frac{\partial \boldsymbol{\xi}}{\partial \boldsymbol{\eta}}\right| d\boldsymbol{\eta}. \tag{13}$$

The probability P_I becomes

$$P_I = \int_{t_0}^{t_0+T} \int_{\Lambda_t} \rho(\mathbf{X}, t; t_0) \left|\mathbf{v}\cdot\hat{\mathbf{r}}\right| d\mathbf{A}_{\Lambda_t}\, dt. \tag{14}$$

Finding the Integration Limits

Now that we have coordinates for Λ_t, we must determine the limits of integration. Looking at Eq. (8), we see that trajectories on Λ_t first meet the range criteria at time t, and not before. Moreover, on those trajectories we must have $dr/dt = \mathbf{v}(t)\cdot\hat{\mathbf{r}}(t) \le 0$. We now adopt two assumptions:

> **Assumption (A1).** *Only one crossing.* Each collision trajectory in V_I meets the criterion $\|\mathbf{r}(t)\| = R$ with $\mathbf{v}(t)\cdot\hat{\mathbf{r}}(t) \le 0$ just once during the time $(t_0, t_0 + T]$.

Assumption (A2). *Trajectories must cross.* No collision trajectories in V_I satisfy $\mathbf{r} = R$ for a finite interval of time. Trajectories either cross at time t with $\mathbf{v}(t) \cdot \hat{\mathbf{r}}(t) < 0$ or are at a local minimum of $\mathbf{r}$ at time t so that $r(t + dt) > R \, \forall dt > 0$ no matter how small.

Comment. One may need to choose t_0, T, and R properly to meet Assumption (A1). This assumption will not be met only in exceptional cases; for example, the assumption should be investigated when the two objects are controlled to move close together for an extended time (i.e., formation flying). We expect Assumption (A2) to be met almost always; if not, one can adjust the value of R to meet the assumption.

Given Assumptions (A1) and (A2), there is only one time t at which $\mathbf{r} = R$ with $\mathbf{v} \cdot \hat{\mathbf{r}} \leq 0$ on each collision trajectory in V_I. Thus, Λ_t is completely known, and the integration limits for P_I can now be specified. The probability P_I becomes

$$P_I = \int_{t_0}^{t_0+T} \int_{0}^{2\pi} \int_{-\frac{\pi}{2}}^{\frac{\pi}{2}} \int_{\mathbf{v}\cdot\hat{\mathbf{r}} \leq 0} \int_{-\infty}^{\infty} \rho(\mathbf{X}, t; t_0) \big|\mathbf{v} \cdot \hat{\mathbf{r}}\big| \, R^2 \cos\theta \, d\mathbf{x}_a \, d\mathbf{v} \, d\theta \, d\phi \, dt \, . \tag{15}$$

Comment. While the term $\mathbf{v} \cdot \hat{\mathbf{r}}$ is a flux term, Eq. (15) does not result from an application of Reynold's transport theorem. Reynold's transport models the time derivative of an extrinsic quantity (e.g., mass) defined as an integral of an intrinsic quantity (e.g., mass density) over a bounded volume. The extrinsic quantity has a value at each time t. The time derivative of the extrinsic quantity at t depends on the transportation of the intrinsic quantity across the volume's surfaces and any generation of the intrinsic quantity within the volume itself. In that computation both influx and outflux must be considered*. In our case, collision probability is defined for a time interval, not at any particular time t. However, one could readily define a concept like 'probability of collision at time t' for which Reynold's transport would apply where of course both influx and outflux would need to be considered. In fact, the discussions from Akella and Alfriend[7] and from Khutorovsky[6] follow along these lines. However, one cannot easily compute the collision probability over a time interval from a probability concept known as a function of time because the collision probability at each time t is correlated in time to its value at nearby times (i.e., values are not independent over time). This a direct result of trajectories moving according to a dynamical model, and not randomly. With the time correlation itself difficult to determine, it is difficult to integrate the proper expression over a time interval to arrive at the correct result.

Modeling Independent Objects

The most typical case involving space objects is that the orbit determination is performed independently for each object and each object's force model is independent of the location of the other object. We make the following assumption:

Assumption (A3). *Independence.* The dynamic model and probability distribution function for each object is independent.

*In contrast, Eq. (15) models only influx, which resulted from identifying trajectories in Ω_t.

Comment. This would not be an appropriate model for objects flying in formation where control acutation was made on one object (e.g., using small thrusters or drag make-up) based upon the location of the other object.

Applying Assumption (A3), the dynamical model of Eq. (1) becomes

$$\frac{d\mathbf{x}_a}{dt} = \mathbf{f}_a(\mathbf{x}_a, t) \; , \mathbf{x}_a(t_0) = \mathbf{x}_{a_0}, \tag{16a}$$

$$\frac{d\mathbf{x}_b}{dt} = \mathbf{f}_b(\mathbf{x}_b, t) \; , \mathbf{x}_b(t_0) = \mathbf{x}_{b_0}. \tag{16b}$$

The combined probability distribution $\rho(\mathbf{X}, t; t_0)$ is computed as

$$\rho(\mathbf{X}, t; t_0) = \rho_a(\mathbf{x}_a, t; t_0)\rho_b(\mathbf{x}_b, t; t_0) = \rho_a(\mathbf{x}_a, t; t_0)\rho_b(\mathbf{x}_a + \mathbf{x}, t; t_0). \tag{17}$$

The probability P_I becomes

$$P_I = \int_{t_0}^{t_0+T} \int_0^{2\pi} \int_{-\frac{\pi}{2}}^{\frac{\pi}{2}} R^2 \cos\theta \int_{\mathbf{v}\cdot\hat{\mathbf{r}} \leq 0} \left|\mathbf{v}\cdot\hat{\mathbf{r}}\right| \int_{-\infty}^{\infty} \rho_a(\mathbf{x}_a, t; t_0)\rho_b(\mathbf{x}_a + \mathbf{x}, t; t_0)\, d\mathbf{x}_a \, d\mathbf{v} \, d\theta \, d\phi \, dt \; . \tag{18}$$

Gaussian Distributions

In many cases, the probability distribution functions ρ_i are approximated as Gaussian distributions. An initially Gaussian distribution will evolve over time as Gaussian for linear dynamical models; the dynamical model for space objects given by Eq. (1), however, is decidedly nonlinear. On the other hand, the error dynamics for the system results from linearizing the dynamical model about the nominal trajectory. An initially Gaussian distribution of the error will remain Gaussian over time because of its linear dynamical model; likewise, the nominal trajectory at every time t represents the mean value of the state error at each time t. The probability distribution of the error dynamics is often used as an approximation to the probability distribution function of the full system, for trajectories that remain near the nominal trajectory. Motivated by these notions, we make the following assumption:

> **Assumption (A4).** *Gaussian distribution.* The probability distribution functions ρ_a and ρ_b remain Gaussian at each time t.

Comment. This assumption means that the means $\boldsymbol{\mu}_a(t)$ and $\boldsymbol{\mu}_b(t)$ and the covariances $\mathbf{P}_a(t)$ and $\mathbf{P}_b(t)$ are known on $t \in [t_0, t_0 + T]$. Certainly, when the equations of motion in Eq. (16) are linear, then the mean and covariance are readily computed as functions of the initial mean, initial covariance and the state transition matrix.

Since the product of two Gaussian distributions is again Gaussian, the expression for P_0 and P_I can be simplified further. Let $\mathcal{N}_n(\boldsymbol{\xi}, \boldsymbol{\eta}, \mathbf{P})$ represent a normal distribution for an n-dimensional variable $\boldsymbol{\xi}$ with mean $\boldsymbol{\eta}$ and covariance matrix $\mathbf{P}$, i.e.,

$$\mathcal{N}_n(\boldsymbol{\xi}, \boldsymbol{\eta}, \mathbf{P}) = \frac{1}{\sqrt{(2\pi)^n}} \frac{1}{\sqrt{\det \mathbf{P}}} \exp\left[-\frac{1}{2}\left(\boldsymbol{\xi} - \boldsymbol{\eta}\right)^T \mathbf{P}^{-1} \left(\boldsymbol{\xi} - \boldsymbol{\eta}\right)\right]. \tag{19}$$

Applying Assumption (A4), we find

$$\rho_a(\mathbf{x}_a, t; t_0) = \mathcal{N}_6(\mathbf{x}_a, \boldsymbol{\mu}_a, \mathbf{P}_a)\ , \quad \rho_b(\mathbf{x}_b, t; t_0) = \mathcal{N}_6(\mathbf{x}_b, \boldsymbol{\mu}_b, \mathbf{P}_b) \tag{20}$$

and*

$$\begin{aligned} \rho_a(\mathbf{x}_a, t; t_0)\rho_b(\mathbf{x}_a + \mathbf{x}, t; t_0) &= \mathcal{N}_6(\mathbf{x}_a, \boldsymbol{\mu}_a, \mathbf{P}_a)\mathcal{N}_6(\mathbf{x}_a + \mathbf{x}, \boldsymbol{\mu}_b, \mathbf{P}_b) \\ &= \mathcal{N}_6(\mathbf{x}_a + \mathbf{T}\mathbf{x}, \boldsymbol{\mu}_a + \mathbf{T}\boldsymbol{\mu}, \mathbf{G})\mathcal{N}_6(\mathbf{x}, \boldsymbol{\mu}, \mathbf{P}) \end{aligned} \tag{21}$$

where $\boldsymbol{\mu} = \boldsymbol{\mu}_b - \boldsymbol{\mu}_a$, $\mathbf{P} = \mathbf{P}_a + \mathbf{P}_b$, $\mathbf{G}^{-1} = \mathbf{P}_a^{-1} + \mathbf{P}_b^{-1}$, and $\mathbf{T} = \mathbf{G}\mathbf{P}_b^{-1}$. Note that the second normal distribution does not depend on $\mathbf{x}_a$.

The expression for P_0 becomes

$$\begin{aligned} P_0 &= \int\limits_{\|\mathbf{r}_0\| \le R} \int\limits_{-\infty}^{\infty} \mathcal{N}_6(\mathbf{x}_0, \boldsymbol{\mu}_0, \mathbf{P}) \int\limits_{-\infty}^{\infty} \mathcal{N}_6(\mathbf{x}_{a_0} + \mathbf{T}\mathbf{x}_0, \boldsymbol{\mu}_{a_0} + \mathbf{T}\boldsymbol{\mu}_0, \mathbf{G}) d\mathbf{x}_{a_0}\, d\mathbf{v}_0\, d\mathbf{r}_0\ , \\ &= \int\limits_{\|\mathbf{r}_0\| \le R} \int\limits_{-\infty}^{\infty} \mathcal{N}_6(\mathbf{x}_0, \boldsymbol{\mu}_0, \mathbf{P}) d\mathbf{v}_0\, d\mathbf{r}_0\ , \end{aligned} \tag{22}$$

where the inner integration becomes 1 because of Lemma III and Lemma V. Using Eq. (21), Lemma III and Lemma V, the expression for P_I given in Eq. (18) becomes

$$P_I = \int\limits_{t_0}^{t_0+T} \int\limits_{0}^{2\pi} \int\limits_{-\frac{\pi}{2}}^{\frac{\pi}{2}} R^2 \cos\theta \int\limits_{\mathbf{v}\cdot\hat{\mathbf{r}} \le 0} \mathcal{N}_6(\mathbf{x}, \boldsymbol{\mu}, \mathbf{P}) \left|\mathbf{v} \cdot \hat{\mathbf{r}}\right| d\mathbf{v}\, d\theta\, d\phi\, dt\ . \tag{23}$$

Integrating Over the Relative Velocity

The integrals in Eq. (22) and Eq. (23) can be further simplified by performing the integration over the relative velocity $\mathbf{v}$. First partition the covariance matrix $\mathbf{P}$ into its 3×3 parts:

$$\mathbf{P} = \begin{vmatrix} \mathbf{A} & \mathbf{B}^T \\ \mathbf{B} & \mathbf{C} \end{vmatrix} \tag{24}$$

where $\mathbf{A}$ and $\mathbf{C}$ are symmetric positive-definite 3×3 matrices. Applying Lemma I of Appendix A, we find

$$\mathcal{N}_6(\mathbf{x}, \boldsymbol{\mu}, \mathbf{P}) = \mathcal{N}_3(\mathbf{r}, \boldsymbol{\mu}_r, \mathbf{A})\mathcal{N}_3(\mathbf{v}', \boldsymbol{\mu}_v', \mathbf{C}')\ , \tag{25}$$

where $\boldsymbol{\mu} = (\boldsymbol{\mu}_{\mathbf{r}}, \boldsymbol{\mu}_{\mathbf{v}})$, $\mathbf{v}' = \mathbf{v} - \mathbf{B}\mathbf{A}^{-1}\mathbf{r}$, $\boldsymbol{\mu}_v' = \boldsymbol{\mu}_v - \mathbf{B}\mathbf{A}^{-1}\boldsymbol{\mu}_r$, and $\mathbf{C}' = \mathbf{C} - \mathbf{B}\mathbf{A}^{-1}\mathbf{B}^T$.

Simplifying P_0. Using Eq. (25) in Eq. (22), we find

$$\begin{aligned} P_0 &= \int\limits_{\|\mathbf{r}_0\| \le R} \mathcal{N}_3(\mathbf{r}_0, \boldsymbol{\mu}_{r_0}, \mathbf{A}_0) \int\limits_{-\infty}^{\infty} \mathcal{N}_3(\mathbf{v}_0', \boldsymbol{\mu}_{v_0}', \mathbf{C}_0') d\mathbf{v}_0'\, d\mathbf{r}_0\ . \\ &= \int\limits_{\|\mathbf{r}_0\| \le R} \mathcal{N}_3(\mathbf{r}_0, \boldsymbol{\mu}_{r_0}, \mathbf{A}_0)\, d\mathbf{r}_0\ , \end{aligned} \tag{26}$$

where Lemma V has again been applied to the inner integral. As expected, the velocity uncertainty completely integrates out of the expression. The expression for P_0 integrates the range uncertainty within the volume of a sphere of radius R using the initial (Gaussian) probability distribution.

*See Appendix C for a derivation of this product of two normal distributions.

Simplifying P_I. The expression for P_I becomes

$$P_I = \int_{t_0}^{t_0+T} \int_0^{2\pi} \int_{-\frac{\pi}{2}}^{\frac{\pi}{2}} R^2 \cos\theta\, \mathcal{N}_3(\mathbf{r}, \boldsymbol{\mu}_r, \mathbf{A}) \nu(\hat{\mathbf{r}}, t)\; d\theta\, d\phi\, dt \tag{27}$$

$$\text{where } \nu(\hat{\mathbf{r}}, t) = \int_{\mathbf{v}'\cdot\hat{\mathbf{r}}+\varepsilon_0(\hat{\mathbf{r}},t)\le 0} \mathcal{N}_3(\mathbf{v}', \boldsymbol{\mu}'_v, \mathbf{C}') \left|\mathbf{v}' \cdot \hat{\mathbf{r}} + \varepsilon_0(\hat{\mathbf{r}}, t)\right| d\mathbf{v}' \,. \tag{28}$$

where $\mathbf{v} \cdot \hat{\mathbf{r}} = \mathbf{v}' \cdot \hat{\mathbf{r}} + \varepsilon_0(\hat{\mathbf{r}}, t)$ with $\varepsilon_0(\hat{\mathbf{r}}, t) = R\,\hat{\mathbf{r}}^T \mathbf{B}\mathbf{A}^{-1}\hat{\mathbf{r}}$. The expression for $\nu(\hat{\mathbf{r}}, t)$ can be found explicitly by first noting that $\hat{\mathbf{r}}$ is just a parameter during this integration (it will be integrated over in the outer integration over A_s). Let $\hat{\mathbf{i}} = (1, 0, 0)$ and define $\mathbf{T}$ so that $\hat{\mathbf{i}} = \mathbf{T}\hat{\mathbf{r}}$. (The choice for $\mathbf{T}$ of course depends on the parameter $\hat{\mathbf{r}}$). Using Lemma IV from Appendix A,

$$\mathcal{N}_3(\mathbf{v}', \boldsymbol{\mu}'_v, \mathbf{C}') = \mathcal{N}_3(\mathbf{v}'', \boldsymbol{\mu}''_v, \mathbf{D}) \tag{29}$$

where $\mathbf{v}'' = \mathbf{T}\mathbf{v}'$, $\boldsymbol{\mu}''_v = \mathbf{T}\boldsymbol{\mu}'_v$, and $\mathbf{D} = \mathbf{T}\mathbf{C}'\mathbf{T}^T$. Partition $\mathbf{D}$ as

$$\mathbf{D} = \begin{vmatrix} \sigma^2 & \mathbf{w}^T \\ \mathbf{w} & \mathbf{E} \end{vmatrix} \quad \text{where } \sigma(\hat{\mathbf{r}}, t) \in \mathbb{R}, \mathbf{w} \in \mathbb{R}^2 \,, \tag{30}$$

with $\sigma(\hat{\mathbf{r}}, t) > 0$ being a scalar and $\mathbf{E}$ a symmetric positive-definite 2×2 matrix. Note that $\sigma(\hat{\mathbf{r}}, t)$ is the standard deviation of the effective relative velocity uncertainty in the $\hat{\mathbf{r}}$ direction, and is completely known from

$$\sigma^2 = \hat{\mathbf{i}}^T \mathbf{D}\hat{\mathbf{i}} = \hat{\mathbf{r}}^T \mathbf{C}'\hat{\mathbf{r}} = \hat{\mathbf{r}}^T \left(\mathbf{C} - \mathbf{B}\mathbf{A}^{-1}\mathbf{B}^T\right) \hat{\mathbf{r}} \,. \tag{31}$$

Applying Lemma I from Appendix A, we find

$$\mathcal{N}_3(\mathbf{v}'', \boldsymbol{\mu}''_v, \mathbf{D}) = \mathcal{N}_1(\varepsilon, \mu_\varepsilon, \sigma^2)\mathcal{N}_2(\boldsymbol{\zeta} - \frac{\varepsilon}{\sigma^2}\mathbf{w}, \boldsymbol{\mu}_\zeta - \frac{\mu_\varepsilon}{\sigma^2}\mathbf{w}, \mathbf{E} - \frac{1}{\sigma^2}\mathbf{w}\mathbf{w}^T) \,, \tag{32}$$

where $\mathbf{v}'' = (\varepsilon, \boldsymbol{\zeta})$ and $\boldsymbol{\mu}''_v = (\mu_\varepsilon, \boldsymbol{\mu}_\zeta)$. The variable μ_ε is completely determined from

$$\mu_\varepsilon = \hat{\mathbf{i}}^T \boldsymbol{\mu}''_v = \hat{\mathbf{i}}^T \mathbf{T}\boldsymbol{\mu}'_v = \hat{\mathbf{r}}^T \left(\boldsymbol{\mu}_v - \mathbf{B}\mathbf{A}^{-1}\boldsymbol{\mu}_r\right) \,. \tag{33}$$

Substituting into Eq. (28), noting that $\hat{\mathbf{r}}^T\mathbf{v}' = \hat{\mathbf{i}}^T\mathbf{T}\mathbf{v}' = \hat{\mathbf{i}}^T\mathbf{v}'' = \varepsilon$, and again using Lemma III and Lemma V,

$$\nu(\hat{\mathbf{r}}, t) = \int_{\varepsilon+\varepsilon_0(\hat{\mathbf{r}},t)\le 0} \mathcal{N}_1(\varepsilon, \mu_\varepsilon, \sigma^2)\left|\varepsilon + \varepsilon_0(\hat{\mathbf{r}}, t)\right| d\varepsilon \,. \tag{34}$$

Noting that on the integration range for ε the term $\varepsilon + \varepsilon_0(\hat{\mathbf{r}}, t) \le 0$, and then simplifying, we find

$$\nu(\hat{\mathbf{r}}, t) = \int_{-\infty}^{-\varepsilon_0(\hat{\mathbf{r}},t)} -\frac{1}{\sqrt{2\pi}\sigma} \left(\varepsilon + \varepsilon_0(\hat{\mathbf{r}}, t)\right) \exp\left[-\frac{(\varepsilon - \mu_\varepsilon)^2}{2\sigma^2}\right] d\varepsilon \,. \tag{35}$$

This is readily integrated analytically as

$$\nu(\hat{\mathbf{r}}, t) = \frac{\sigma(\hat{\mathbf{r}}, t)}{\sqrt{2\pi}} H(\tilde{\nu}) \,, \tag{36a}$$

$$H(\tilde{\nu}) = e^{-\tilde{\nu}^2} - \sqrt{\pi}\tilde{\nu}\left(1 - \text{erf}(\tilde{\nu})\right) \,, \tag{36b}$$

$$\tilde{\nu} = \frac{\nu_0(\hat{\mathbf{r}}, t)}{\sqrt{2}\sigma(\hat{\mathbf{r}}, t)} \,, \tag{36c}$$

where $\nu_0(\hat{\mathbf{r}}, t) = \varepsilon_0(\hat{\mathbf{r}}, t) + \mu_\varepsilon$, expressed in the original variables, is

$$\nu_0(\hat{\mathbf{r}}, t) = \hat{\mathbf{r}}^T \left[\boldsymbol{\mu}_v + \mathbf{B}\mathbf{A}^{-1}\left(R\hat{\mathbf{r}} - \boldsymbol{\mu}_r\right)\right] \,. \tag{37}$$

Comment. The condition $\mathbf{v} \cdot \hat{\mathbf{r}} \leq 0$ defines a half-infinite space with a planar boundary. The transformations made above create a pair of coordinates that are parallel to the planar boundary and one coordinate perpendicular to it. The integration for the pair is then over an infinite plane and integrates to 1; the integration for the other coordinate is over a half-infinite line. The variables $\sigma(\hat{\mathbf{r}}, t)$, $\nu(\hat{\mathbf{r}}, t)$, and $\nu_0(\hat{\mathbf{r}}, t)$ each have the dimension of velocity. A plot of $H(\tilde{\nu})$ shows that it monotonically decreases* as $\tilde{\nu}$ increases and $H(\tilde{\nu}) \to 0$ as $\tilde{\nu} \to \infty$; it is positive for all $\tilde{\nu}$. Thus, $\nu(\hat{\mathbf{r}}, t)$ is positive for all $\nu_0(\hat{\mathbf{r}}, t)$.

Summary

The formula for the probability of collision between two objects, meeting Assumptions (A1), (A2), (A3), and (A4) is given by $P = P_0 + P_I$ where

$$P_0 = \int_0^R \int_0^{2\pi} \int_{-\frac{\pi}{2}}^{\frac{\pi}{2}} \mathcal{N}_3\left(\mathbf{r}_0, \boldsymbol{\mu}_r(t_0), \mathbf{A}(t_0)\right)\; r_0^2 \cos\theta \, d\theta \, d\phi \, dr_0 \,, \tag{38a}$$

$$P_I = \int_{t_0}^{t_0+T} \int_0^{2\pi} \int_{-\frac{\pi}{2}}^{\frac{\pi}{2}} \mathcal{N}_3(\mathbf{r}, \boldsymbol{\mu}_r(t), \mathbf{A}(t))\nu(\hat{\mathbf{r}}, t)\; R^2 \cos\theta \, d\theta \, d\phi \, dt \,, \tag{38b}$$

where $\boldsymbol{\mu}_r(t)$ is the mean relative position, $\mathbf{A}(t)$ is the covariance of the relative position, $\nu(\hat{\mathbf{r}}, t)$ is defined by Eq. (36), and (θ, ϕ) are spherical coordinates parameterizing $\hat{\mathbf{r}}$. The integral for P_0 involves the volume of a sphere; the integral for P_I is the integral on the surface of a sphere over the time interval being considered.

Extension for Non-Gaussian distributions

Recently, there has been much interest in better approximating the probability density function for nonlinear dynamical systems, where Assumption (A4) is not used. One approach is the use of a Gaussian mixture model[13] where the probability density function is represented as a weighted sum of Gaussian distributions. In that case, the formula developed in Eq. (38) can be readily extended.

REDUCTION TO THE CLASSIC SHORT ENCOUNTER FORMULA

The classic short encounter formula for the probability of collision between space objects has been derived by many authors.[1,4,2,7] In the derivations, the motion of the objects is modeled by Eq. (16) (using a very simple choice for $\mathbf{f}_i$) meeting Assumption (A3). The probability density function is modeled as Gaussian meeting Assumption (A4). Assumptions (A1) and (A2) are met as a consequence of the motion described below in Assumption (A6).

*The derivative $dH/d\tilde{\nu} = \sqrt{\pi}\left(\text{erf}(\tilde{\nu}) - 1\right)$ is negative for all $\tilde{\nu}$.

Velocity Uncertainty

In addition to the assumptions already made above, three new key assumptions are made. The first new assumption is

> **Assumption (A5).** *No Velocity Uncertainty.* The velocity uncertainty is zero, rendering ρ_a and ρ_b as being functions only of position and time.

Comment. This assumption means that the initial relative velocity $\mathbf{v}_0$ is known precisely, though the initial relative position $\mathbf{r}_0$ is still uncertain. While perturbed trajectories all have the same *initial* relative velocity $\mathbf{v}_0$, they may have different relative velocity $\mathbf{v}$ at later times, depending on the dynamical model given in Eq. (16). Trajectories with initial conditions within the range R of the mean initial condition will only stay within R over time if the divergence of the vector field $\mathbf{f}_b - \mathbf{f}_a$ is non-positive (i.e., volume elements do not expand over time). Moreover, if the divergence is negative, then volume elements contract over time and it is possible that a trajectory initially outside the range R will become within R at some later time.

As a consequence of Assumption (A5), the combined covariance matrix $\mathbf{P}$ is only concerned with the 3×3 matrix $\mathbf{A}$. To apply this assumption to the general result, we take $\mathbf{B} \to 0$ and $\sigma \to 0^+$ (since σ was derived in a manner requiring $\sigma > 0$). Then $\nu_0(\hat{\mathbf{r}}, t)$ in Eq. (37) becomes $\boldsymbol{\mu}_v \cdot \hat{\mathbf{r}}$. The limit as $\sigma \to 0^+$ of the exponential term in Eq. (36b) is zero but the other term takes some care. Since $\hat{\mathbf{r}}$ is an integration variable whose integration limits span the entire surface of a sphere, $\nu_0(\hat{\mathbf{r}}, t)$ can be positive, negative or zero. When $\nu_0(\hat{\mathbf{r}}, t)$ is zero, the limit of the second term in Eq. (36b) is zero. When $\nu_0(\hat{\mathbf{r}}, t)$ is positive, erf() $\to 1$ and the limit is zero. When $\nu_0(\hat{\mathbf{r}}, t)$ is negative, erf() $\to -1$, and

$$\lim_{\sigma \to 0^+} \nu(\hat{\mathbf{r}}, t) = -\nu_0(\hat{\mathbf{r}}, t) = -\boldsymbol{\mu}_v \cdot \hat{\mathbf{r}} \; , \quad \text{when } \nu_0(\hat{\mathbf{r}}, t) \leq 0 \; . \tag{39}$$

The integration limits for (ϕ, θ) can now be restricted to the hemisphere where $\boldsymbol{\mu}_v \cdot \hat{\mathbf{r}} \leq 0$. Since t is just a parameter during the integration over a sphere, we can choose t-dependent axes for the spherical coordinates that align the x-axis with $\boldsymbol{\mu}_v$. Then the integral can be expressed as

$$P_I = -\int_{t_0}^{t_0+T} \int_{\frac{\pi}{2}}^{\frac{3\pi}{2}} \int_{-\frac{\pi}{2}}^{\frac{\pi}{2}} \mathcal{N}_3(\mathbf{r}, \boldsymbol{\mu}, \mathbf{A})(\boldsymbol{\mu}_v \cdot \hat{\mathbf{r}}) \; R^2 \cos\theta \, d\theta \, d\phi \, dt \; . \tag{40}$$

This would agree with Eq.(26) from Akella and Alfriend[7] and with Eq.(2) from Khutorovsky et al.[6] except they incorrectly indicate to integrate over the entire sphere, not just a hemisphere*.

Short Encounter Time

The next key assumption is that the encounter occurs over such a small time interval that certain approximations are valid:

> **Assumption (A6).** *Short Encounter Time.* The time interval over which the encounter takes place is small enough that

*In subsequent equations, both derivations actually only integrate over a hemisphere, arriving at the correct result.

i. The motion of each object can be well-approximated as a straight line.

ii. The combined covariance is constant in time.

Comment. Taken together, Assumptions (A5) and (A6i) imply that all perturbed trajectories have the *same* constant relative velocity $\mathbf{v} = \mathbf{v}_0$ over time. Moreover, the vector field in Eq. (16) has no divergence and trajectories do not move apart from each other. In fact, trajectories for a sphere of initial conditions with $\mathbf{r}_0 \leq R$ centered on the mean trajectory sweep out a cylinder over time, often referred to as the collision tube. Only trajectories starting within the tube can ever collide; no trajectory outside the tube ever crosses inside. The probability of collision formula can be derived using this property of the tube; however, in more general situations where the divergence is not zero, a tube swept out by initial conditions within a sphere of radius R does not represent the only trajectories that could have a collision.

The straight-line approximation combines with Assumption (A5) to require that $\mathbf{f}_i = (\mathbf{v}_{i_0}, 0)$ in Eq. (16), resulting in $d\mathbf{r}/dt = \mathbf{v}_0$, making the solution for the mean trajectory

$$\boldsymbol{\mu}_r(t) = \boldsymbol{\mu}_{r_0} + \boldsymbol{\mu}_{v_0}(t - t_0) = \boldsymbol{\mu}_{r_0} + \mathbf{v}_0(t - t_0) \; . \tag{41}$$

For this system, with the velocity uncertainty zero, it can easily be shown that the relative position covariance remains constant in time.

Integrating over the Encounter Time

We can further simplify Eq. (40) by noting that since $\boldsymbol{\mu}_v = \mathbf{v}_0$, $\mathbf{v}_0 = v_0\, \hat{\mathbf{i}}$. In that case,

$$\mu_x(t) = \mu_{x_0} + v_0(t - t_0) \; , \tag{42a}$$

$$\mu_y(t) = \mu_{y_0} \; , \tag{42b}$$

$$\mu_z(t) = \mu_{z_0} \; . \tag{42c}$$

The integral over the hemispherical area can be performed by instead integrating over the cross-sectional area A_c perpendicular to $\mathbf{v}_0$ (i.e., with normal $\hat{\mathbf{i}}$ and coordinates y and z*). Note that we must take $x \leq 0$ when integrating over $\mathbf{r} = (x, y, z)$ to properly represent the integral over the correct hemisphere. The probability integral becomes

$$P_I = \int_{t_0}^{t_0+T} \iint_{A_c} \mathcal{N}_3(\mathbf{r}, \boldsymbol{\mu}_r, \mathbf{A}_0) v_0 \; dydzdt \; . \tag{43}$$

where we have used $dy\, dz = R^2 \cos^2\theta \cos\phi \, d\theta \, d\phi = R^2 \cos\theta \, d\theta \, d\phi \, |\hat{\mathbf{i}} \cdot \hat{\mathbf{r}}|$ and $\hat{\mathbf{i}} \cdot \hat{\mathbf{r}} \leq 0$. This agrees with Eq.(28) of Akella and Alfriend[7] though they integrate over all time rather than adhering to a short time duration. Following them, we apply Lemma II, letting $\mathbf{r} = (x, \boldsymbol{\zeta})$ with $\boldsymbol{\zeta} = (y, z)$ and

$$\mathbf{A}_0 = \begin{vmatrix} \eta^2 & \mathbf{w}^T \\ \mathbf{w} & \mathbf{P}_c \end{vmatrix} \qquad \eta \in \mathbb{R}, \mathbf{w} \in \mathbb{R}^2 \; . \tag{44}$$

We find

$$\begin{aligned} \mathcal{N}_3(\mathbf{r}, \boldsymbol{\mu}_r, \mathbf{A}_0) \;\; &= \;\; \mathcal{N}_1(x - \mathbf{w}^T \mathbf{P}_c^{-1} \boldsymbol{\zeta}, \mu_x - \mathbf{w}^T \mathbf{P}_c^{-1} \boldsymbol{\mu}_\zeta, \sigma_\nu^2) \mathcal{N}_2(\boldsymbol{\zeta}, \boldsymbol{\mu}_\zeta, \mathbf{P}_c), \\ \text{where } \sigma_\nu^2 \;\; &= \;\; \eta^2 - \mathbf{w}^T \mathbf{P}_c^{-1} \mathbf{w} \; . \end{aligned} \tag{45}$$

*Actually, Eq. (40) integrates over the left hemisphere whose normal is $-\hat{\mathbf{i}}$.

Note $\boldsymbol{\mu}_\zeta = \boldsymbol{\mu}_{\zeta_0}$ is a constant over time given Eq. (42), and that the second normal distribution in Eq. (45) is independent of time t. The probability integral is then

$$P_I = \iint\limits_{|\boldsymbol{\zeta}|\le R} \mathcal{N}_2(\boldsymbol{\zeta}, \boldsymbol{\mu}_{\zeta_0}, \mathbf{P}_c) \int\limits_{t_0}^{t_0+T} \mathcal{N}_1(x - \mathbf{w}^T\mathbf{P}_c^{-1}\boldsymbol{\zeta}, \mu_x - \mathbf{w}^T\mathbf{P}_c^{-1}\boldsymbol{\mu}_{\zeta_0}, \sigma_\nu^2) v_0 \, dt \, d\boldsymbol{\zeta} \; , \tag{46}$$

where $x = -\sqrt{R^2 - \boldsymbol{\zeta}\cdot\boldsymbol{\zeta}}$ and μ_x is given in Eq. (42a). The inner integral is an integral over time t, treating $\boldsymbol{\zeta}$ as a parameter, where the only time dependence lies in μ_x, and simplifies to

$$\int\limits_{t_0}^{t_0+T} \mathcal{N}_1 \, v_0 \, dt \; = \int\limits_{\chi_0}^{\chi_T} \mathcal{N}_1(\chi, 0, \sigma_\nu^2) \, d\chi \; , \tag{47a}$$

$$\text{where } \chi = v_0(t - t_0) + \mathbf{w}^T\mathbf{P}_c^{-1}(\boldsymbol{\zeta} - \boldsymbol{\mu}_{\boldsymbol{\zeta}_0}) + \sqrt{R^2 - \boldsymbol{\zeta}\cdot\boldsymbol{\zeta}} + \mu_{x_0} \; . \tag{47b}$$

Even though the encounter is assumed to be of short duration, the time integration is usually performed over all time (or equivalently, for $\chi \in (-\infty, \infty)$ in Eq. (47a)), and using Lemma III and Lemma V the integral is 1. From a computational perspective, the duration T need not be infinite; it just needs to be long enough to make the the integral approximately 1. The relevant time scale is $\Delta t = \sigma_\nu / v_0$, and the integral will be approximately 1 for $T \simeq N\,\Delta t$, for an integer N not too large. Several authors[3,5] describe the time integration as instead an integration along the axis of the collision tube using a distance measure related to χ.

The Short Encounter Formula

We now make two additional assumptions:

> **Assumption (A7).** *Time integrates out.* The time integration interval is sufficiently long to approximate the time integral as 1, but not so long as to violate the short encounter assumption (A6).

Comment. Assumption (A7) is a somewhat odd assumption. Its effect is to simplify the resulting expression.

> **Assumption (A8).** *Initial probability is negligible.* The time t_0 can be chosen to make $P_0 \approx 0$.

Comment. Assumption (A8) is satisfied whenever there exists a time t_0 at which the objects are widely separated. This assumption would need to be investigated for objects that remain close at all time, i.e., objects in formation.

Using all assumptions, we find

$$P \simeq P_I = \iint\limits_{|\boldsymbol{\zeta}|\le R} \mathcal{N}_2(\boldsymbol{\zeta}, \boldsymbol{\mu}_{\zeta_0}, \mathbf{P}_c) d\boldsymbol{\zeta} \; , \tag{48}$$

which is the classic formula for the probability of collision for short encounters. The computation takes place over the interior of a circle of radius R where the plane of the circle is perpendicular to the relative velocity $\mathbf{v}_0$. This is referred to as the encounter plane when the velocity $\mathbf{v}_0$ is taken to be the relative velocity at TCA. The covariance $\mathbf{P}_c$ is the combined covariance of the relative position projected into this plane.

RESULTS

We compare the value obtained from the probability of collision formula defined by Eq. (38) with Monte Carlo results for a selection of test cases created by Sal Alfano.[11] Alfano published a set of test cases that compared the results of Monte Carlo simulation with several short-term and long-term probability of collision formulas. In the tests, the mean motion $(\boldsymbol{\mu}_r(t), \boldsymbol{\mu}_v(t))$ was approximated as the difference in the nominal motions* of the two objects and the probability density function was approximated as being Gaussian about this mean motion, with the covariance being propagated in time using the appropriate linear time-update law. Often, millions of simulations would need to be run to insure statistically significant Monte Carlo results.

Routines were written in MATLAB to compute P_0 and P_I given a table of ephemerides that included 6×6 covariance matrices. The grid of ephemeris data was generated by STK† by numerically integrating the trajectory and the covariance matrix. When computing P_I, the time integration was performed first, using Simpson's rule; the integration over the sphere was done using a high-order Lebedev[12] method available from MathWorks. Likewise, when computing P_0, the radial integration was performed first using Simpson's rule and the integration over the sphere was performed using Lebedev's method. Lebedev's method was computed using 1454 samples, though the results are not appreciably different when using 2030 or 5810 samples. MATLAB is not particularly well-suited for fast computations, yet the typical computational time was only about 30 secs: the exception was test case 10 which needed 10 secs steps to achieve accuracy and took 2 minutes to compute.

Test case 3 involves a short-term encounter of GEO objects for which the classic formula works well. All 10 methods assessed by Alfano for this case produce results within 0.5%–1.0% of the Monte Carlo value of 0.100846. We compute a value of 0.100424 (a difference of -0.4%) using Eq. (38) for the time interval $[-8, 8]$ sec, where $t = 0$ represents the TCA. The time step used for the time integration was set at 0.1 sec to insure enough samples to achieve accuracy (the results were off by 10% using a step of 1.0 sec). At $t_0 = -8$, the initial probability P_0 is zero and the probability accumulates over the conjunction interval because of trajectories having a collision at a later time.

It is instructive to see how the probability is affected by the choice of time interval. We divided the original interval $[-8, 8]$ into two parts: the left interval $[-8, t^\flat]$ and the right interval $[t^\flat, 8]$ for various $t^\flat$ and compiled the results listed in Table 1. One can see that the initial probability P_0 is greatest at TCA (see P_0 for the right interval at $t^\flat = 0$). The impacting trajectories are much more probable before TCA (see the increase of P_I for the left interval) than after TCA (see the nearly zero value for P_I for the right interval for $t^\flat \geq 0$). The probability P for the right interval decreases as $t^\flat$ increases because trajectories that collided at earlier times are not considered: the exception is the value listed at $t^\flat = -0.8$. That time is near the time of the most probable impacting trajectory and is more sensitive to the time step used in performing the integration. Figure 2 shows the effect of step sized selection for one sample point on the sphere. Using a step size of 0.01 sec, the conjunction probability is computed to be 0.100287, and the value of P for the right interval always decreases as $t^\flat$ increases.

A much better test of Eq. (38) involves long-term encounters where the assumptions required by short-term formula are not met. Four examples from Alfano are shown in Table 2. In each case, the TCA corresponds to $t = 0$. Of all the methods compared by Alfano, the voxel method[10] was closest

*The nominal motion is the trajectory corresponding to the mean initial condition.

†Software available from Analytical Graphics Inc., www.agi.com.

Table 1. Results for a Short-Term Encounter: Test Case 3

$t^\flat$ (sec)	Left Interval P_0	Left Interval P_I	Left Interval P	Right Interval P_0	Right Interval P_I	Right Interval P
-1.0	0.0	0.004367	0.004367	0.004387	0.096057	0.100443
-0.8	0.0	0.041028	0.041028	0.040762	0.059396	0.100158
-0.6	0.0	0.073343	0.073343	0.073219	0.027080	0.100299
-0.4	0.0	0.089232	0.089232	0.089098	0.011192	0.100289
-0.2	0.0	0.097368	0.097368	0.097230	0.003056	0.100287
0.0	0.0	0.100170	0.100170	0.099778	0.000254	0.100031
0.2	0.0	0.100422	0.100422	0.097219	0.000002	0.097221
0.4	0.0	0.100424	0.100424	0.089086	0.000000	0.089086
0.6	0.0	0.100424	0.100424	0.073309	0.000000	0.073309
0.8	0.0	0.100424	0.100424	0.040578	0.000000	0.040578
1.0	0.0	0.100424	0.100424	0.003301	0.000000	0.003301

to the Monte Carlo results, which involves the numerical integration of many trajectories. Alfano recommends that voxels only be used in reference cases because of the computational complexity and slow computation speed. In all cases shown in Table 2, the probability P computed using Eq. (38) is more accurate than even voxels and computes quickly. For test case 11, Alfano re-ran the Monte Carlo simulation to count collisions exactly as this paper defines. The Monte Carlo and voxel results listed in the table for test case 11 have been updated from his original paper. Only one million simulations were run for this new simulation, however, so the confidence of this Monte Carlo result is less than in the other test cases.

Table 2. Comparison with Monte Carlo Results: Long-Term Encounters

Test Case	Orbit Type	Step (sec)	t_0 (sec)	$t_0 + T$ (sec)	Conjunction Probability: Monte Carlo	Conjunction Probability: P	Conjunction Probability: Voxels	% Difference: P	% Difference: Voxels
4	GEO	60.0	-21600	21600	0.073090	0.073643	0.073900	0.75	1.11
8	MEO	60.0	-10135	10135	0.035256	0.035201	0.035134	-0.16	-0.35
10	HEO	10.0	-14400	14400	0.362952	0.364002	0.366169	0.29	0.89
11	LEO	60.0	-1420	1420	0.004452	0.004320	0.003841	-2.92	-13.72

FURTHER WORK

One caveat in using Alfano's test cases is that all the tests have very small velocity uncertainty. Even near TCA, the velocity remains sufficiently small that Assumption (A5) is met and P_I can be computed using the simpler formula given by Eq. (40) with little change in the results. More work needs to be done to create test cases with realistic velocity uncertainty (i.e., values typically found for objects as a result of the orbit determination process) where statistically significant Monte Carlo results have been computed.

CONCLUSIONS

We have derived a probability of collision formula from first principles, including both position and velocity uncertainty, identifying all the relevant assumptions along the way. The formula applies under very mild assumptions; in particular, no assumptions are made about the relative motion nor constancy of the covariance. We have showed that the formula reduces to the classic short encounter

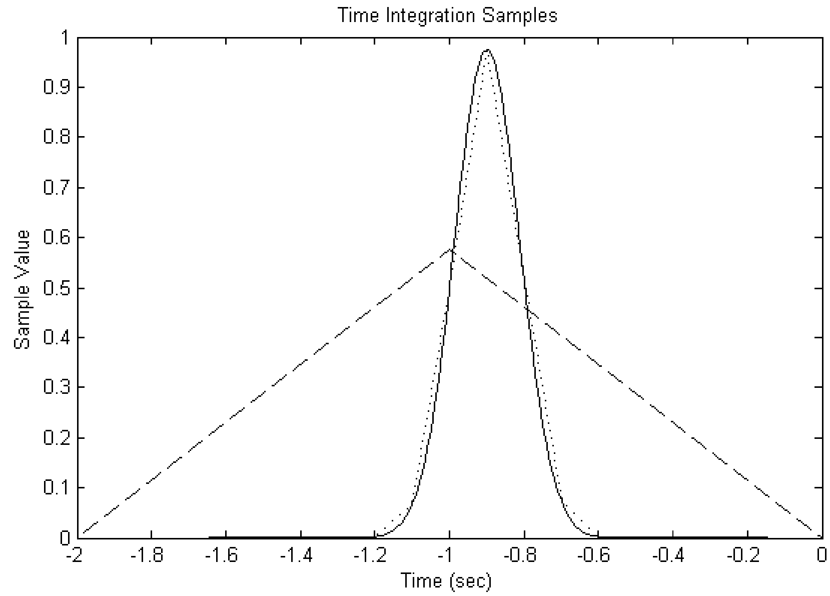

Figure 2. The effect of step size selection on time integration for one sample point on the sphere. The dashed line shows samples at 1 sec; the dotted line at 0.1 sec; and the solid line at 0.01 sec.

formula under the requisite assumptions. Comparisons to Monte Carlo simulations show excellent agreement in both short-term and long-term encounters and can be computed much faster than previously proposed methods.

ACKNOWLEDGMENT

The author would like to thank Sergei Tanygin, Frank Stoner, and Jim Woodburn for their many helpful comments on the paper; Sal Alfano for his development of the test cases, especially his re-running of test case 11; and Prof. Akella for his help with understanding his paper.

APPENDIX A PROPERTIES OF GAUSSIAN DISTRIBUTION FUNCTIONS

Let $\mathcal{N}_n(\boldsymbol{\xi}, \boldsymbol{\eta}, \mathbf{P})$ represent a normal distribution for an n-dimensional variable $\boldsymbol{\xi}$ with mean $\boldsymbol{\eta}$ and covariance matrix $\mathbf{P}$, a symmetric positive definite $n \times n$ matrix, i.e.,

$$\mathcal{N}_n(\boldsymbol{\xi}, \boldsymbol{\eta}, \mathbf{P}) = \frac{1}{\sqrt{(2\pi)^n}} \frac{1}{\sqrt{\det \mathbf{P}}} \exp\left[-\frac{1}{2} (\boldsymbol{\xi} - \boldsymbol{\eta})^T \mathbf{P}^{-1} (\boldsymbol{\xi} - \boldsymbol{\eta}) \right]. \tag{A1}$$

Consider a partitioning of $\boldsymbol{\xi}$, $\boldsymbol{\eta}$, and $\mathbf{P}$ where $\boldsymbol{\xi} = (\boldsymbol{\varepsilon}, \boldsymbol{\zeta})$, $\boldsymbol{\eta} = (\boldsymbol{\eta}_\varepsilon, \boldsymbol{\eta}_\zeta)$ and

$$\mathbf{P} = \begin{vmatrix} \mathbf{R} & \mathbf{Q}^T \\ \mathbf{Q} & \mathbf{S} \end{vmatrix}, \tag{A2}$$

where $\boldsymbol{\varepsilon}$ and $\boldsymbol{\eta}_\varepsilon$ are r-dimensional, $\boldsymbol{\zeta}$ and $\boldsymbol{\eta}_\zeta$ are s-dimensional, $\mathbf{Q}$ is $s \times r$, $\mathbf{R}$ is a symmetric positive definite $r \times r$ matrix, $\mathbf{Q}$ is a symmetric positive-definite $s \times s$ matrix, and $n = r + s$.

Lemma I.

$$\begin{aligned} \mathcal{N}_n(\boldsymbol{\xi}, \boldsymbol{\eta}, \mathbf{P}) &= \mathcal{N}_r(\boldsymbol{\varepsilon}, \boldsymbol{\eta}_\varepsilon, \mathbf{R}) \mathcal{N}_s(\boldsymbol{\zeta} + \mathbf{T}\boldsymbol{\varepsilon}, \boldsymbol{\eta}_\zeta + \mathbf{T}\boldsymbol{\eta}_\varepsilon, \mathbf{S}'), \\ \text{where } \mathbf{S}' &= \mathbf{S} - \mathbf{Q}\mathbf{R}^{-1}\mathbf{Q}^T \\ \text{and } \mathbf{T} &= -\mathbf{Q}\mathbf{R}^{-1}. \end{aligned}$$

Proof. Define $\boldsymbol{\xi}' = (\boldsymbol{\varepsilon}', \boldsymbol{\zeta}') = \mathbf{M}\boldsymbol{\xi}$ where the linear transformation matrix $\mathbf{M}$ is

$$\mathbf{M} = \begin{vmatrix} \mathbf{I}_r & \mathbf{0}_{rs} \\ \mathbf{T} & \mathbf{I}_s \end{vmatrix}. \tag{A3}$$

Note that $\mathbf{M}$ is invertible and has determinant 1. The transformation leaves $\boldsymbol{\varepsilon}$ unaltered (i.e., $\boldsymbol{\varepsilon}' = \boldsymbol{\varepsilon}$). Define $\boldsymbol{\eta}' = \mathbf{M}\boldsymbol{\eta}$ analogously. Under the transformation, the quadratic form in $\mathcal{N}_6(\boldsymbol{\xi}, \boldsymbol{\eta}, \mathbf{P})$ becomes

$$\exp\left[-\frac{1}{2}(\boldsymbol{\xi} - \boldsymbol{\eta})^T \mathbf{P}^{-1} (\boldsymbol{\xi} - \boldsymbol{\eta})\right] = \exp\left[-\frac{1}{2}\left(\boldsymbol{\xi}' - \boldsymbol{\eta}'\right)^T \mathbf{M}^{-T}\mathbf{P}^{-1}\mathbf{M}^{-1}\left(\boldsymbol{\xi}' - \boldsymbol{\eta}'\right)\right] \tag{A4}$$

leading us to define $\mathbf{P}' = \mathbf{M}\mathbf{P}\mathbf{M}^T$ where

$$\mathbf{P}' = \begin{vmatrix} \mathbf{R} & \mathbf{0} \\ \mathbf{0} & \mathbf{S}' \end{vmatrix} \tag{A5}$$

Note that $\det \mathbf{P} = \det \mathbf{P}' = \det \mathbf{R} \det \mathbf{S}'$. Because $\mathbf{P}'$ is trivially inverted, the quadratic form becomes

$$\begin{aligned} \exp\left[-\frac{1}{2}(\boldsymbol{\xi} - \boldsymbol{\eta})^T \mathbf{P}^{-1} (\boldsymbol{\xi} - \boldsymbol{\eta})\right] &= \exp\left[-\frac{1}{2}\left(\boldsymbol{\xi}' - \boldsymbol{\eta}'\right)^T \mathbf{P}'^{-1}\left(\boldsymbol{\xi}' - \boldsymbol{\eta}'\right)\right] \\ &= \exp\left[-\frac{1}{2}(\boldsymbol{\varepsilon} - \boldsymbol{\eta}_\varepsilon)^T \mathbf{R}^{-1} (\boldsymbol{\varepsilon} - \boldsymbol{\eta}_\varepsilon)\right] \\ &\quad \times \exp\left[-\frac{1}{2}\left(\boldsymbol{\zeta}' - \boldsymbol{\eta}'_\zeta\right)^T \mathbf{S}'^{-1}\left(\boldsymbol{\zeta}' - \boldsymbol{\eta}'_\zeta\right)\right]. \end{aligned} \tag{A6}$$

Now from the transformation $\boldsymbol{\zeta}' = \boldsymbol{\zeta} + \mathbf{T}\boldsymbol{\varepsilon}$ and $\boldsymbol{\eta}'_\zeta = \boldsymbol{\eta}_\zeta + \mathbf{T}\boldsymbol{\eta}_\varepsilon$, completing the proof. ∎

Lemma II.

$$\begin{aligned} \mathcal{N}_n(\boldsymbol{\xi}, \boldsymbol{\eta}, \mathbf{P}) &= \mathcal{N}_r(\boldsymbol{\varepsilon} + \mathbf{T}^T\boldsymbol{\zeta}, \boldsymbol{\eta}_\varepsilon + \mathbf{T}^T\boldsymbol{\eta}_\zeta, \mathbf{R}') \mathcal{N}_s(\boldsymbol{\zeta}, \boldsymbol{\eta}_\zeta, \mathbf{S}), \\ \text{where } \mathbf{R}' &= \mathbf{R} - \mathbf{Q}^T\mathbf{S}^{-1}\mathbf{Q} \\ \text{and } \mathbf{T} &= -\mathbf{S}^{-1}\mathbf{Q}. \end{aligned}$$

Proof. This follows similarly to Lemma I, where

$$\mathbf{M} = \begin{vmatrix} \mathbf{I}_r & \mathbf{T}^T \\ \mathbf{0}_{sr} & \mathbf{I}_s \end{vmatrix}. \tag{A7}$$

■

Lemma III.

$$\mathcal{N}_n(\boldsymbol{\xi}+\boldsymbol{\varpi},\boldsymbol{\eta},\mathbf{P}) = \mathcal{N}_n(\boldsymbol{\xi},\boldsymbol{\eta}-\boldsymbol{\varpi},\mathbf{P}) = \mathcal{N}_n(\boldsymbol{\xi}+\boldsymbol{\varpi}-\boldsymbol{\eta},\mathbf{0},\mathbf{P}) \tag{A8}$$

Proof. Follows from direct computation. ■

Lemma IV.

$$\mathcal{N}_3(\boldsymbol{\xi},\boldsymbol{\eta},\mathbf{P}) = \mathcal{N}_3(\mathbf{T}\boldsymbol{\xi},\mathbf{T}\boldsymbol{\eta},\mathbf{T}\mathbf{P}\mathbf{T}^T) \tag{A9}$$

Proof. Follows from direct computation. ■

Lemma V.

$$\int_{-\infty}^{\infty} \mathcal{N}_n(\boldsymbol{\xi},\boldsymbol{\varpi},\mathbf{P})\, d\boldsymbol{\xi} = 1 \tag{A10}$$

for any constant value $\boldsymbol{\varpi}$ whether it is the mean of $\boldsymbol{\xi}$ or not.
Proof. From Lemma III, $\mathcal{N}_n(\boldsymbol{\xi},\boldsymbol{\varpi},\mathbf{P}) = \mathcal{N}_n(\boldsymbol{\xi}-\boldsymbol{\varpi},0,\mathbf{P}) = \mathcal{N}_n(\boldsymbol{\xi}',0,\mathbf{P})$ where the integration limits remain over all space since $\boldsymbol{\varpi}$ is a constant parameter. By definition, integration of this last expression over all space is 1. ■

APPENDIX B PROBABILITY DENSITY FUNCTIONS

Let $\boldsymbol{\xi}$ be a random variable with probability density function $\rho_{\boldsymbol{\xi}}(\boldsymbol{\xi})$. The probability density function has the property that for any domain V of $\boldsymbol{\xi}$, the probability that $\boldsymbol{\xi} \in V$ is

$$P(\boldsymbol{\xi} \in V) = \int_V \rho_{\boldsymbol{\xi}}(\boldsymbol{\xi}) d\boldsymbol{\xi}. \tag{B1}$$

Invariance under transformation

The value of an integral is independent of the coordinates with which it is computed. Let $\boldsymbol{\xi} = \boldsymbol{\Phi}(\boldsymbol{\eta},t)$ be a t-parametric transformation of variables from $\boldsymbol{\eta}$ to $\boldsymbol{\xi}$, where $\boldsymbol{\Phi}$ is a invertible continuous function with continuous partial derivatives. Let $\Psi(\boldsymbol{\xi},t)$ represent the inverse of $\boldsymbol{\Phi}$. The volume elements are related by the Jacobian of the transformation $\mathbf{J} = \partial\boldsymbol{\Phi}/\partial\boldsymbol{\eta}$ according to

$$d\boldsymbol{\xi} = |\det\mathbf{J}|\, d\boldsymbol{\eta}. \tag{B2}$$

Define U_t as the transformation of V, i.e., $U_t = \Psi(V,t)$. Then

$$P(\boldsymbol{\xi} \in V) = \int_{U_t} \rho_{\boldsymbol{\xi}}(\boldsymbol{\Phi}(\boldsymbol{\eta},t))|\det\mathbf{J}(\boldsymbol{\eta},t)|\, d\boldsymbol{\eta} = \int_{U_t} \rho_{\boldsymbol{\eta}}(\boldsymbol{\eta},t) d\boldsymbol{\eta} = P(\boldsymbol{\eta} \in U_t), \tag{B3}$$

where

$$\rho_{\boldsymbol{\eta}}(\boldsymbol{\eta},t) \triangleq \rho_{\boldsymbol{\xi}}\left(\boldsymbol{\Phi}(\boldsymbol{\eta},t)\right)) \left|\det\mathbf{J}(\boldsymbol{\eta},t)\right|. \tag{B4}$$

Obviously, $\rho_{\boldsymbol{\eta}}(\boldsymbol{\eta},t)$ satisfies the properties of a probability density function for $\boldsymbol{\eta}$ at each parameter value t. Thus, the probability contained within a differential volume is invariant under the transformation, i.e.,

$$\rho_{\boldsymbol{\xi}}(\boldsymbol{\xi})d\boldsymbol{\xi} = \rho_{\boldsymbol{\eta}}(\boldsymbol{\eta},t)d\boldsymbol{\eta}. \tag{B5}$$

Time-evolution

Let $\boldsymbol{\eta} = \boldsymbol{\Psi}(\boldsymbol{\xi}, t)$ represent the t-parametric transformation of variables defined by the solution to the differential equation

$$\frac{d\boldsymbol{\eta}}{dt} = \mathbf{F}(\boldsymbol{\eta}, t) \ , \ \boldsymbol{\eta}(t_0) = \boldsymbol{\xi}, \tag{B6}$$

with $\mathbf{F}$ being continuous with continuous partial derivatives, and bounded on some domain W. Then solutions to Eq. (B6) exist and are unique on W. Moreover, the Jacobian $\mathbf{K} = \partial\boldsymbol{\Psi}/\partial\boldsymbol{\xi}$ is not singular on solutions in W (i.e., $\det \mathbf{K} \neq 0$) and since $\mathbf{K}(\boldsymbol{\xi}, t_0)$ is the identity matrix, $\det \mathbf{K} > 0$ on all solutions in W. Since $\mathbf{J} = \mathbf{K}^{-1}$ and the determinant of the inverse is the reciprocal, Eq. (B4) becomes

$$\rho_{\boldsymbol{\xi}}(\boldsymbol{\xi}) = \rho_{\boldsymbol{\eta}}(\boldsymbol{\Psi}(\boldsymbol{\xi}, t), t) \det \mathbf{K}(\boldsymbol{\xi}, t) \ . \tag{B7}$$

Differentiating with respect to time t, using Jacobi's formula for the derivative of the determinant, and simplifying, we find

$$\begin{aligned} 0 &= \left(\frac{\partial \rho_{\boldsymbol{\eta}}}{\partial t} + \frac{\partial \rho_{\boldsymbol{\eta}}}{\partial \boldsymbol{\eta}} \frac{\partial \boldsymbol{\Psi}}{\partial t} \right) \det \mathbf{K} + \rho_{\boldsymbol{\eta}} \det \mathbf{K} \, \nabla_{\boldsymbol{\eta}} \cdot \mathbf{F} \ , && \text{(B8)} \\ &= \frac{\partial \rho_{\boldsymbol{\eta}}}{\partial t} + \nabla_{\boldsymbol{\eta}} \rho_{\boldsymbol{\eta}} \cdot \mathbf{F} + \rho_{\boldsymbol{\eta}} \, \nabla_{\boldsymbol{\eta}} \cdot \mathbf{F} \ , && \text{(B9)} \\ &= \frac{\partial \rho_{\boldsymbol{\eta}}}{\partial t} + \nabla_{\boldsymbol{\eta}} \cdot (\rho_{\boldsymbol{\eta}} \mathbf{F}) \ . && \text{(B10)} \end{aligned}$$

Like Eq. (B7), Eq. (B10) expresses the conservation (or continuity) of probability. It is a PDE for $\rho_{\boldsymbol{\eta}}(\boldsymbol{\eta}, t)$ with boundary condition $\rho_{\boldsymbol{\eta}}(\boldsymbol{\eta}, t_0) = \rho_{\boldsymbol{\xi}}(\boldsymbol{\xi})$. This is just the deterministic part of the Kolmogorov forward equation (KFE)*. The KFE models the time-evolution of the probability density function for systems modeled using stochastic differential equations.†

APPENDIX C PRODUCT OF TWO NORMAL DISTRIBUTIONS

Consider the product ρ of two normal distributions of the same dimension n of the form

$$\rho = \mathcal{N}_n(\mathbf{x}_a, \boldsymbol{\mu}_a, \mathbf{P}_a) \mathcal{N}_n(\mathbf{x}_a + \mathbf{x}, \boldsymbol{\mu}_b, \mathbf{P}_b) \ . \tag{C1}$$

ρ can be refactored into two other normal distributions where one is independent of $\mathbf{x}_a$. Let $\boldsymbol{\xi} = \mathbf{x}_a - \boldsymbol{\mu}_a$ and $\boldsymbol{\eta} = \mathbf{x} - \boldsymbol{\mu}$ with $\boldsymbol{\mu} = \boldsymbol{\mu}_b - \boldsymbol{\mu}_a$. Then by Lemma III

$$\rho = \mathcal{N}_n(\boldsymbol{\xi}, 0, \mathbf{P}_a) \, \mathcal{N}_n(\boldsymbol{\xi} + \boldsymbol{\eta}, 0, \mathbf{P}_b) \ . \tag{C2}$$

The exponential term appearing in Eq. (C2) becomes

$$\exp \left[-\frac{1}{2} \left\{ \boldsymbol{\xi}^T \mathbf{P}_a^{-1} \boldsymbol{\xi} + (\boldsymbol{\xi} + \boldsymbol{\eta})^T \mathbf{P}_b^{-1} (\boldsymbol{\xi} + \boldsymbol{\eta}) \right\} \right] \ . \tag{C3}$$

Direct computation shows that the inner expression can be factored as

$$(\boldsymbol{\xi} + \mathbf{T}\boldsymbol{\eta})^T \mathbf{G}^{-1} (\boldsymbol{\xi} + \mathbf{T}\boldsymbol{\eta}) + \boldsymbol{\eta}^T \mathbf{P}_b^{-1} \left(\mathbf{I}_n - \mathbf{T} \right) \boldsymbol{\eta} \ , \tag{C4a}$$

$$\text{where} \quad \mathbf{G}^{-1} = \mathbf{P}_a^{-1} + \mathbf{P}_b^{-1} \ , \tag{C4b}$$

*Also known by the name Fokker-Planck equation (FPE).

†See Reference 14 for a discussion.

$\mathbf{T} = \mathbf{G}\mathbf{P}_b^{-1}$ and $\mathbf{I}_n$ is the $n \times n$ identity matrix. Now $\mathbf{P}_b^{-1}(\mathbf{I}_n - \mathbf{T}) = \mathbf{P}_b^{-1} - \mathbf{P}_b^{-1}\mathbf{G}\mathbf{P}_b^{-1}$, and applying the matrix inversion lemma* we find

$$\left(\mathbf{P}_b^{-1}(\mathbf{I}_n - \mathbf{T})\right)^{-1} = \mathbf{P}_b + (\mathbf{G}^{-1} - \mathbf{P}_b^{-1})^{-1} = \mathbf{P}_b + \mathbf{P}_a \triangleq \mathbf{P}\ . \tag{C5}$$

Therefore the exponential argument can be written

$$(\boldsymbol{\xi} + \mathbf{T}\boldsymbol{\eta})^T\mathbf{G}^{-1}(\boldsymbol{\xi} + \mathbf{T}\boldsymbol{\eta}) + \boldsymbol{\eta}^T\mathbf{P}^{-1}\boldsymbol{\eta}\ . \tag{C6}$$

Now consider the determinant of $\mathbf{P}$:

$$\det\mathbf{P} = \det\mathbf{P}_a \det\mathbf{P}_b \det(\mathbf{P}_a^{-1} + \mathbf{P}_b^{-1}) \ = \det\mathbf{P}_a \det\mathbf{P}_b \det\mathbf{G}^{-1}\ . \tag{C7}$$

Since the determinant of the inverse is the reciprocal,

$$\det\mathbf{P}_a \det\mathbf{P}_b = \det\mathbf{P} \det\mathbf{G} \tag{C8}$$

Thus using Lemma III,

$$\rho = \mathcal{N}_n(\boldsymbol{\xi} + \mathbf{T}\boldsymbol{\eta}, 0, \mathbf{G})\,\mathcal{N}_n(\boldsymbol{\eta}, 0, \mathbf{P}) = \mathcal{N}_n(\mathbf{x}_a + \mathbf{T}\mathbf{x}, \boldsymbol{\mu}_a + \mathbf{T}\boldsymbol{\mu}, \mathbf{G})\,\mathcal{N}_n(\mathbf{x}, \boldsymbol{\mu}, \mathbf{P})\ . \tag{C9}$$

REFERENCES

[1] J. L. Foster and H. S. Estes, "A Parametric Analysis of Orbital Debris Collision Probability and Maneuver Rate for Space Vehicles," *NASA/JSC-25898*, Aug. 1992.

[2] K. Chan, "Collision Probability Analyses for Earth Orbiting Satellites," *Adv. Astro. Sci.*, Vol. 96, 1997, pp. 1033–1048.

[3] K. Chan, *Spacecraft Collision Probability*. El Segundo, CA.: The Aerospace Corporation, 2008.

[4] S. Alfano, "Determining Satellite Close Approaches," *J. Astron. Sci.*, Vol. 41, No. 2, 2005, pp. 217–225.

[5] S. Alfano, "A Numerical Implementation of Spherical Object Collision Probability," *J. Astron. Sci.*, Vol. 53, No. 1, 2005, pp. 103–109.

[6] Z. N. Khutorovsky, V. F. Boikov, and S. Y. Kamensky, "Direct Method for the Analysis of Collision Probability of Artificial Space Objects in LEO: Techniques, Results, and Applications," *Proc. First European Conf. on Space Debris*, Apr. 1993, pp. 491–508.

[7] M. R. Akella and K. T. Alfriend, "Probability of Collision Between Space Objects," *J. GCD*, Vol. 23, No. 5, 2000, pp. 769–772.

[8] R. P. Patera, "General Method for Calculating Satellite Collision Probability," *AIAA J. GCD*, Vol. 24, No. 4, 2001, pp. 716–722.

[9] D. Oltrogge and R. Gist, "Collision Vision Situational Awareness for Safe and Reliable Space Operations," *50th Intern. Astron. Congress*, Oct. 1999.

[10] S. Alfano, "Addressing Nonlinear Relative Motion for Spacecraft Collision Probability," *AAS/AIAA Astrodynamics Specialist Conference*, Keystone, CO., Paper 2006-6760, Aug. 2006.

[11] S. Alfano, "Satellite Conjunction Monte Carlo Analysis," *AAS Spaceflight Mechanics Mtg*, Pittsburgh, PA., Paper 09-233, Feb. 2009.

[12] V. Lebedev and D. Laikov, "A quadrature formula for the sphere of the 131st algebraic order of accuracy," *Doklady Mathematics*, Vol. 59, No. 3, 1999, pp. 477–481. Other citations are available for lower orders. Wikipedia has a discussion under the term 'Lebedev quadrature.' MATLAB code is available at www.mathworks.com.

[13] D. Giza, P. Singla, and M. Jah, "An Approach for Nonlinear Uncertainty Propagation: Application to Orbital Mechanics," *AIAA Guidance, Navigation, and Control Conference*, Chicago IL., Aug. 2009.

[14] J. L. Crassidis and J. L. Junkins, *Optimal Estimation of Dynamic Systems*. Boca Raton, FL.: CRC Press, 2nd ed., 2012.

* $(\mathbf{A} + \mathbf{B}\mathbf{C}\mathbf{D})^{-1} = \mathbf{A}^{-1} - \mathbf{A}^{-1}\mathbf{B}\left(\mathbf{D}\mathbf{A}^{-1}\mathbf{B} + \mathbf{C}^{-1}\right)^{-1}\mathbf{D}\mathbf{A}^{-1}$, see Reference 14.